Received: 29 September 2021 | Revised: 20 December 2021 | Accepted: 19 January 2022

DOI: 10.1002/ima.22713

RESEARCH ARTICLE

WILEY

A novel threshold score based multiclass segmentation technique for brain magnetic resonance images using adaptive opposition slime mold algorithm

Manoj Kumar Naik[1] | **Rutuparna Panda**[2] | **Leena Samantaray**[3] | **Ajith Abraham**[4,5]

[1]Faculty of Engineering and Technology, Siksha O Anusandhan, Bhubaneswar, Odisha, India

[2]Department of Electronics and Telecommunication Engineering, Veer Surendra Sai University of Technology, Burla, Odisha, India

[3]Department of Electronics and Communication Engineering, Ajay Binay Institute of Technology, Cuttack, Odisha, India

[4]Machine Intelligence Research Labs, Scientific Network for Innovation and Research Excellence, Auburn, Washington, USA

[5]Center for Artificial Intelligence, Innopolis University, Innopolis, Russia

Correspondence
Rutuparna Panda, Department of Electronics and Telecommunication Engineering, Veer Surendra Sai University of Technology, Burla, Odisha-768018, India.
Email: r_ppanda@yahoo.co.in

Funding information
The Analytical Center for the Government of the Russian Federation, Grant/Award Numbers: IGK000000D730321P5Q0002, 70-2021-00143 dd. 01.11.2021

Abstract

Clinicians can detect diseases early, thanks to the digital image processing methodologies, which improve health together with the treatment experience. The technology of magnetic resonance imaging (MRI) is frequently employed in the brain, research for any kind of related illness. The brain MR image requires precise automated thresholding for a meaningful representation to aid doctors, because of its different modalities and complexity. The majority of the threshold selection strategies are based on entropy. However, these strategies are limited by their reliance on the spatial distribution of gray values. There is also a pressing need to develop a thresholding technique that is independent of the spatial distribution, making it more suitable for a variety of modalities and complexity, such as the brain MR images. A novel non-entropic maximizing objective function for the multilevel thresholding approach using a threshold score (TS) is presented in this paper, to address these concerns. An evolutionary TS-AOSMA approach, using the optimizer called adaptive opposition slime mold algorithm (AOSMA), is suggested to lower the computational cost of TS-based multiclass segmentation, which is a novel idea. The proposed approach is evaluated on T2-weighted brain MR imaging slices from Harvard Medical School's whole brain atlas dataset. When compared to the state-of-the-art Kapur's, Tsallis, and Masi entropy-based technologies, the proposed scheme offered better quantitative and qualitative outcomes. The recommended strategies may be useful in medical image analysis.

KEYWORDS

brain MR image, evolutionary computing, multilevel thresholding, slime mold algorithm

1 | INTRODUCTION

Medical imaging allows clinicians to detect diseases early on, resulting in better patient outcomes. For a healthier society, a proper medical image analysis, to help clinicians, is required. Due to the modern medical equipment with faster processing speed, the medical image analysis using image processing techniques via computer vision is now extremely successful. Segmenting the image into usable findings, also known as image segmentation, is one of the most essential challenges in the medical image analysis. The image segmentation techniques are

successfully applied in the medical image analysis for the brain.[1] The magnetic resonance imaging (MRI) is the most commonly used type of brain imaging among the four most common types, including computerized tomography (CT), MRI, electroencephalography (EEG), and positron emission tomography (PET). It is due to its lack of radiation exposure, low invasiveness, and widespread availability.[2] Another benefit of MRI is that it provides more information about the soft tissues with a better contrast.[3] The abbreviations are listed below in Table 1 for better readability.

The most prevalent method of segmentation is through thresholding.[4] An efficient thresholding technique, when applied to a brain MRI, can have a significant impact on the results of finding lesions or disorders within the image. The global thresholding methods are described in References,[4–6] with the Otsu between class variance technique,[7] Shannon entropy method,[8] Tsallis entropy method,[9] Kapur's entropy method,[10] cross-entropy method,[11] Masi entropy method[12] being the most common among the researchers. Thresholding is a method of separating one or more foreground objects from the background in an image using a similarity approach.

TABLE 1 Abbreviations with their descriptions

MRI	Magnetic resonance imaging
TS	Threshold score
AOSMA	Adaptive opposition slime mold algorithm
CT	Computerized tomography
EEG	Electroencephalography
PET	Positron emission tomography
BFOA	Bacterial foraging optimization algorithm
TLBO	Teaching learning based optimization
CSA	Crow search algorithm
ABF	Adaptive bacterial foraging
RCGA	Real coded genetic algorithm
SBX	Simulated binary crossover
MPSO	Mutation-based particle swarm optimization
AWDO	Adaptive wind driven optimization
SMA	Slime mold algorithm
TS-AOSMA	Threshold score-based optimal multilevel thresholding using AOSMA
PSNR	Peak signal to noise ratio
SSIM	Structure similarity index
FSIM	Feature similarity index
TH	Threshold
MSE	Mean square error
AVE	Average
OPT	Optimal

Broadly, the thresholding methods are classified into the bi-level and the multilevel. The bi-level thresholding divides the image into two classes by using a single threshold value $(K = 1)$, whereas the multilevel thresholding divides the image into several classes by using multiple threshold values $(K > 1)$. In practice, the bi-level threshold selection performance is highly inefficient for extracting relevant information, leading to multiclass thresholding. The image histogram is among the most widely used tools in the global thresholding strategy,[4] which employs L distinct gray levels and their frequencies in an image. The approach of determining the K threshold levels is an exhaustive search with a computational cost of $O(L^K)$.[13] As a result, a primary disadvantage of multilevel thresholding is that it is computationally inefficient when compared to bi-level thresholding because it requires more computation. As a result, as K increases, so does the computational complexity.

The above research work, more or less, has concentrated on the use of entropy-based fitness (objective) functions. These technologies are dependent on the image histograms. Therefore, they suffer from the non-uniform distribution of the gray values. Further, the computation burden increases, when the number of threshold levels K increases. Further, the idea of opposition-based learning was never integrated into optimizers. The existing optimization algorithms are, thus, offering us a limited exploration of the search space.

In the earlier technologies, bi-level thresholding was used to segment the MRI into two regions. The bi-level segmented image was then used for the analysis. However, limited features are found in a bi-level segmented image. Therefore, there is a strong need to extend the idea of bi-level segmentation into a multilevel segmentation, resulting in a multiclass segmented output. Interestingly, more features are found in a multiclass segmented (output) image of an MRI, which is essential for analysis. The output attained is the multiclass segmented output.

An optimization strategy can be utilized to discover the threshold value more rapidly to address the issue of the high computing cost, in the exhaustive search of the multilevel thresholding, in the brain MR images. The following are some significant research outcomes on the brain MR image thresholding that use the basic version optimization techniques: bacterial foraging optimization algorithm (BFOA), teaching learning-based optimization (TLBO)[14] and crow search algorithm (CSA).[15] The basic version of the optimization method is inadequate for all types of difficulties, prompting the hybridization of algorithms or the modification of the search strategy to get a more effective multilevel thresholding performance on the brain MR images. Some applications in the brain MR image thresholding reported, using the hybrid/modified optimization algorithms, are as follows: adaptive

bacterial foraging (ABF),[16] real coded genetic algorithm (GA) using simulated binary crossover (SBX),[17] mutation-based particle swarm optimization (MPSO),[18] modified particle swarm optimization[19] and adaptive wind-driven optimization (AWDO).[20] These basic/hybrid/modified optimization algorithms are used in the histogram-based multilevel thresholding such as Otsu's methods,[16,18,20] Kapur's entropy,[1,14,16,17,20] Shannon entropy,[14] Tsallis entropy[14] and cross entropy.[15] The above discussions prompted us to develop a unique objective function for multilevel thresholding. Then use an efficient pre-approved optimizer to tackle the concerns of the computational cost.

The spatial distribution of the intensity values influences the performances of the histogram-based multilevel thresholding techniques. As a result, when there is a substantial variation in the intensity values in an image, segmentation accuracy suffers. This has motivated us to develop a firsthand threshold score (TS)-based maximization criterion objective function for the multilevel thresholding that overcomes the limitation of the spatial variation of the intensity values. The concept begins with the bi-level thresholding and subsequently progresses to multilevel thresholding. This addition may help to expand the multilevel thresholding literature in the image processing field. Because most research on the brain MR image multilevel thresholding relies on the histogram of the MR image. In this work, we exploit the thresholding using a non-histogram-based approach that is independent of the spatial intensity variations. Further, the proposed adaptive opposition slime mold method (AOSMA)[21] is used as an optimizer for the multilevel thresholding to reduce the computational cost, because it demonstrated good performances and convergence characteristics when compared to other prominent optimizers. This work proposes TS-AOSMA, which stands for threshold score-based evolutionary brain MR image multilevel thresholding utilizing the AOSMA. We employed T2-weighted brain MR imaging slices from Harvard Medical School's whole brain atlas dataset[22] for the experimental purposes in this investigation, because these images are more suited for the brain MRI segmentation.[23] The Tsallis entropy, Kapur's entropy, and Masi entropy-based evolutionary thresholding using AOSMA are also proposed for performance comparison. The suggested evolutionary TS-AOSMA brain MR image multilevel thresholding method is validated. Our suggested methodology produced promising results based on several evaluation criteria for the quantitative analysis and the threshold images for the qualitative analysis.

In summary, this paper developed a new non-entropic objective function, for the first time. New technology in terms of the non-entropic objective function is developed firsthand. The investigated technology is used for MR image segmentation for analysis. The work is compared with state-of-the-art technologies. This may enrich the literature and inspire researchers to work more in this direction.

The key contributions and novelties are

- A non-entropic-based objective (fitness) function is investigated.
- A novel optimizer called AOSMA is proposed for the first time in the literature.
- A firsthand threshold score-based adaptive opposition slime mold technology is fostered for segmentation of the brain MR images.
- Its performances in terms of convergence and accuracy are compared with the state-of-the-art technologies and found better than the other existing methods.

The following is a breakdown of the paper's structure. Section 1 is dedicated to the introduction. Section 2 briefly describes the material and methods used to formulate the problem. Section 3 suggests a new threshold score (TS) based objective function for the multilevel thresholding. Section 4 develops the evolving TS-AOSMA multilevel thresholding scheme. Section 5 focuses on the experimental results. Section 6 describes the final concluding statement.

2 | MATERIAL AND METHODS

2.1 | Multilevel thresholding

Thresholding is the process of segmenting the image into various classes to reduce the complexity of interpreting the information content. Let us consider an image I formed by a $P \times Q$ number of pixels with the intensity value l from an $[l_{\max} - l_{\min} + 1]$ distinct gray levels, within the range $[l_{\min}, l_{\max}]$, where P is the number of rows and Q is the number of columns in the spatial dimensions. The multilevel thresholding is a problem of segmenting the image into multiple classes. So, if the image is classified into $K+1$ number of classes such as $\{M_0, M_1, ..., M_K\}$, we require K number of the threshold values $\{t_1, t_2, ..., t_K\}$ and it must satisfy the condition $t_1 < t_2 < \cdots < t_K$. The multiple classes $\{M_0, M_1, ..., M_K\}$ are classified as follows:

$$\begin{aligned} M_0 &\leftarrow l \quad \text{if } l_{\min} \le l < t_1 \\ M_1 &\leftarrow l \quad \text{if } t_1 \le l < t_2 \\ &\vdots \qquad\qquad \vdots \\ M_K &\leftarrow l \quad \text{if } t_K \le l < l_{\max}, \end{aligned} \tag{1}$$

and

$$I = \bigcup_{c=0}^{K} M_c. \quad (2)$$

The thresholds must be established from $[l_{\max} - l_{\min} - 1]$ (i.e., $[(l_{\max} - 1) - (l_{\min} + 1) + 1]$. This is due to the exclusion of the boundary values $l_{\min}$ and $l_{\max}$, distinct gray levels, which can be considered as an optimization problem based on the design variables $\{t_1, t_2, ..., t_K\}$. The optimal thresholds $\{t_1^*, t_2^*, ..., t_K^*\}$ using a maximization criterion based on the multilevel thresholding objective function (f) is determined as follows:

$$\{t_1^*, t_2^*, ..., t_K^*\} = \arg \max_{0 < t_1 < t_2 < \cdots < t_K < (L-1)} f(t_1, t_2, ..., t_K). \quad (3)$$

Let the individual gray level l probability (p_l) in the target image is:

$$p_l = \frac{n_l}{P \times Q},\ l = (0, 1, ..., L-1), \quad (4)$$

where n_l represents the count of pixels with the intensity value l and $\sum_{l=0}^{L-1} p_l = 1$.

The class probability (ω_i) for the ith class is evaluated as follows:

$$\omega_i = \sum_{l=t_i}^{t_{i+1}-1} p_l, \quad i = (0, 1, ..., K), t_0 = 0 \text{ and } t_{K+1} = L - 1. \quad (5)$$

In this section, we also describe Kapur's,[10] Tsallis[24] and Masi[25] multilevel thresholding objective functions used for comparison.

2.1.1 | Kapur's multilevel thresholding objective function

Kapur's multilevel thresholding utilizes the maximization criterion of the entropy[10] to obtain the optimal thresholds $\{t_1^*, t_2^*, ..., t_K^*\}$. Kapur's multilevel thresholding objective function is given as follows:

$$f_{\text{Kapur}}(t_1, t_2, ..., t_K) = \sum_{i=0}^{K} E_i, \quad (6)$$

where,

$$E_i = -\sum_{l=t_i}^{t_{i+1}-1} \frac{p_l}{\omega_i} \ln \frac{p_l}{\omega_i},\ 0 \le i \le K. \quad (7)$$

2.1.2 | Tsallis multilevel thresholding objective function

Tsallis multilevel thresholding[24] uses the pseudo additive entropy maximization criterion to find the optimal thresholds $\{t_1^*, t_2^*, ..., t_K^*\}$ for a non-extensive statistically independent system. Tsallis multilevel thresholding objective function is given as follows:

$$f_{\text{Tsallis}}(t_1, t_2, ..., t_K) = \sum_{i=0}^{K} H_i^q + (1-q) \prod_{j=0}^{K} H_i^q. \quad (8)$$

The q is the Tsallis parameter (or entropic index) and prior Tsallis for each distributed class is defined as follows:

$$H_i^q = \frac{1}{q-1} \left[1 - \sum_{l=t_i}^{t_{i+1}-1} \left(\frac{p_l}{\omega_i} \right)^q \right], \quad 0 \le i \le K. \quad (9)$$

2.1.3 | Masi multilevel thresholding objective function

Masi multilevel thresholding[25] was used to find the optimal thresholds $\{t_1^*, t_2^*, ..., t_K^*\}$ based on the framework of a maximization criterion of the generalized entropy introduced by Masi.[12] Masi multilevel thresholding objective function is given as follows:

$$f_{\text{Masi}}(t_1, t_2, ..., t_K) = \sum_{i=0}^{K} S_i^r. \quad (10)$$

The r is the Masi parameter (or entropic parameter) and Masi entropy $\left(S_i^r\right)$ for the ith class is calculated as follows:

$$S_i^r = \frac{1}{1-r} \left[\log \left(1 - (1-r) \sum_{l=t_i}^{t_{i+1}-1} \frac{p_l}{\omega_i} \log \frac{p_l}{\omega_i} \right) \right], \quad 0 \le i \le K. \quad (11)$$

2.2 | Adaptive opposition slime mold algorithm

The AOSMA is recently proposed by Naik et al.[21] to enhance the convergence and performance of the slime

mold algorithm.[26] The AOSMA uses an adaptive way to decide when to use the opposition-based learning needs in the SMA to get better optimal results. The AOSMA is inspired by the oscillation mode of the plasmodial slime mold (*Physarum ploycephalum*) and the positive–negative feedback to choose the best-connected food path.

2.2.1 | Mathematical formulation of the AOSMA

The AOSMA process has five major subparts, such as initialization, oscillation, approaching and wrapping foods, adaptive opposition-based learning.

Initialization

As with most optimization algorithms, the AOSMA requires random initialization to initiate the optimization procedure. The initial populations are formulated based on S number of slime molds for d-dimensional problems, within the search space specified by the upper (UB) and the lower (LB) boundary. The random initialization of the population is performed as follows:

$$X_i(\text{itr}) = \text{LB} + \text{rand}_i(1,d) * (\text{UB} - \text{LB}), \quad \forall i \in [1,S], \tag{12}$$

and

$$X(\text{itr}) = \begin{bmatrix} X_1 \\ X_2 \\ \vdots \\ X_S \end{bmatrix}, \tag{13}$$

where ith slime mold position at iteration itr is $X_i \left(= \left\{x_i^1, x_i^2, ..., x_i^d\right\}\right)$, d-dimensional random vector with values from the interval $[0,1]$ is $\text{rand}_i(1,d)$ and for the initialization process itr is consider as 1.

Fitness evaluation and extraction of necessary parameters

The slime molds are evaluated based on the fitness (odor) $f(X_i), \forall i = [1,S]$ for the iteration itr, where itr will be from 1 to maximum iteration Maxitr. The fitness values in a vector $f(= [f(X_1), f(X_2), ..., f(X_S)])$ are sorted in an ascending order for a minimization problem:

$$[\text{SortedFitness}, \text{SortedIndex}] = \text{sort}(f). \tag{14}$$

Based on the sorted fitness value for the iteration (itr), some important parameters like the local best position X_{LB}, local best fitness $f_{\text{LB}}(= f(X_{\text{LB}}))$, local worst fitness f_{LW}, global best fitness f_{GB} and global best position X_{GB}. The above-said parameters are extracted as follows:

$$f_{\text{LB}} = f(\text{SortedFitness}(1)). \tag{15}$$

$$X_{\text{LB}} = X(\text{SortedIndex}(1)). \tag{16}$$

$$f_{\text{LW}} = f(\text{SortedFitness}(S)). \tag{17}$$

$$f_{\text{GB}} = \begin{cases} f_{\text{LB}} & \text{if itr} = 1 \\ f_{\text{LB}} & \text{if itr} > 1 \text{ and} f_{\text{GB}} > f_{\text{LB}} \\ f_{\text{GB}} & \text{if itr} > 1 \text{ and} f_{\text{GB}} \le f_{\text{LB}}. \end{cases} \tag{18}$$

$$X_{\text{GB}} = \begin{cases} X_{\text{LB}} & \text{if itr} = 1 \\ X_{\text{LB}} & \text{if itr} > 1 \text{ and} f_{\text{GB}} > f_{\text{LB}} \\ X_{\text{GB}} & \text{if itr} > 1 \text{ and} f_{\text{GB}} \le f_{\text{LB}} \end{cases}. \tag{19}$$

Oscillation

The oscillation stimulates randomness in the search process to achieve a good trade-off between the exploitation and the exploitation. The oscillation in the AOSMA is governed by a weight W, velocity V_b and V_c.

The weight W is used to imitate the slime mold oscillation frequency, which varies depending on the quality of the food, such as quick for the high-quality food and sluggish for the low-quality food. The W for S slime molds can be modeled as follows:

$$W(\text{SortedIndex}(i)) = \begin{cases} 1 + \text{rand}() * \log\left(\dfrac{f_{\text{LB}} - f(X_i)}{f_{\text{LB}} - f_{\text{LW}}}\right) & 1 \le i \le \dfrac{S}{2} \\ 1 - \text{rand}() * \log\left(\dfrac{f_{\text{LB}} - f(X_i)}{f_{\text{LB}} - f_{\text{LW}}}\right) & \dfrac{S}{2} < i \le S \end{cases}. \tag{20}$$

where rand() is a randomly chosen number between [0,1]. The V_b and V_c are random velocity values selected from a continuous uniform distribution in the intervals $[-b,b]$ and $[-c,c]$. The b and c are determined using the current iteration itr and the maximum iteration Maxitr as follows:

$$b = \text{arctanh}\left(-\left(\frac{\text{itr}}{\text{Maxitr}}\right) + 1\right). \tag{21}$$

and

$$c = 1 - \frac{\text{itr}}{\text{Maxitr}}. \tag{22}$$

Approaching and wrapping foods

The slime mold approaching and wrapping food in the AOSMA is formulated as follows:

$$X\text{new}_i(\text{itr}) = \begin{cases} X_{\text{LB}}(\text{itr}) + V_b(W * X_{\text{LB}}(\text{itr}) - X_R(\text{itr})) & \text{if } r_1 \geq z \text{ and } r_2 < p_i \\ V_c * X_i(\text{itr}) & \text{if } r_1 \geq z \text{ and } r_2 \geq p_i \\ \text{LB} + \text{rand}(1,d) * (\text{UB} - \text{LB}) & \text{if } r_1 < z \end{cases}. \quad (23)$$

The X_R is a slime mold from the S population that has been randomly pooled. The z is the chance of wrapping food to a random search space which is fixed at 0.03. The r_1 and r_2 are two random numbers drawn within the range of $[0,1]$. The p_i, a threshold value is used to determine whether the slime mold will follow the local best slime or its course. The p_i is evaluated as follows:

$$p_i = \tanh|f(X_i) - f_{\text{GB}}|, \forall i \in [1,S] \quad (24)$$

Adaptive opposition-based learning

The AOSMA used an adaptive judgment mechanism to evaluate whether the opposition-based learning (OBL)[27] was required during the search process. The opposite position of a smile mold jth $(\forall j \in [1,d])$ dimension is estimated as follows:

$$X\text{newo}_i^j = \min(X\text{new}_i(\text{itr})) + \max(X\text{new}_i(\text{itr})) - X\text{new}_i^j, \ \forall i \in [1,S] \text{ and } \forall j \in [1,d]. \quad (25)$$

The next iteration's slime mold position is modeled as follows:

$$X_i(\text{itr}+1) = \begin{cases} X\text{new}_i(\text{itr}) \text{ if } f(X\text{new}_i(\text{itr})) < f(X_i(\text{itr})) \\ X\text{sel}_i(\text{itr}) \text{ if } f(X\text{new}_i(\text{itr})) \geq f(X_i(\text{itr})) \end{cases}, \forall i \in [1S]. \quad (26)$$

where $X\text{sel}_i$ is the ith selected position among new position $X\text{new}_i$ and its corresponding opposite position $X\text{newo}_i$, which can be chosen as follows:

$$X\text{sel}_i(\text{itr}) = \begin{cases} X\text{new}_i(\text{itr}) & \text{if } f(X\text{new}_i(\text{itr})) < f(X\text{newo}_i(\text{itr})) \\ X\text{newo}_i(\text{itr}) & \text{if } f(X\text{new}_i(\text{itr})) \geq f(X\text{newo}_i(\text{itr})) \end{cases}, \forall i \in [1,S]. \quad (27)$$

2.2.2 | Pseudocode of the AOSMA

At the outset, determine the number of slime molds S to be used, the objective function f in a d-dimensional issue, the search space boundary UB and LB, and the maximum permitted iteration count as Maxitr. The AOSMA pseudocode looks like this (Algorithm 1):

3 | THE PROPOSED THRESHOLD SCORE (TS) BASED MULTILEVEL THRESHOLDING TECHNIQUE

A novel theoretical research is being conducted here. To prove that our strategy is superior to the entropic value-based methods, we propose a new thresholding function. The problem statement's empirical formulation is described below.

Begin with the bi-level thresholding, in which a threshold t differentiates the image I into two distinct classes M_0 and M_1. If the image I has $P \times Q$ number of pixels with the intensity value $l_{m,n}$ at the spatial coordinates (m,n), where index $m \in (1,2,...,P)$ and

ALGORITHM 1 AOSMA pseudocode

Inputs: N, d, Maxitr, z, f, UB and LB.
Initialization: Initialize itr = 1 and N slime mold using Equations (12) and (13).
while (itr < Maxitr)
  Evaluate the fitness vector f and sort them in ascending order (i.e., minimization problem) using Equation (14).
  Extract and update the necessary parameters such as f_{LB}, X_{LB}, f_{LW}, f_{GB} and X_{GB} using Equations (15–19).
  Update the oscillation parameter weight W, velocity V_b and V_c using Equations (20–22).
 for $i = 1$: S number of slime mold
    Evaluate p_i using Equation (24)
    Generate r_1 and r_2.
    Randomly polled a slime mold X_R for the S population.
    Estimate $X\text{new}_i$ using Equation (23).
   if $(f(X\text{new}_i) > f(X_i))$
     Estimate $X\text{newo}_i$ using Equation (25).
     and select $X\text{sel}_i$ using Equation (27).
   end (if)
   Update the slime mold position X_i for next iterations using Equation (26).
  end (for)
  itr = itr + 1
end (while)
Outputs: f_{GB} and X_{GB}.

$n \in (1,2,...,Q)$. The intensity value $l_{m,n}$, distributed to class M_0 and M_1 based on the threshold t, is given as follows:

$$\begin{matrix} M_0 \leftarrow l_{m,n} & if\ l_{\min} \le l_{m,n} < t_1 \\ M_1 \leftarrow l_{m,n} & if\ t_1 \le l_{m,n} \le l_{\max} \end{matrix}, m \in (1,2,...,P) \text{ and } n \in (1,2,...,Q), \tag{28}$$

which must satisfy $M_0 \cup M_1 = I$.

Let us propose a threshold score (TS) for the bi-level thresholding at a threshold value t as follows:

$$\begin{aligned} \mathrm{TS}(t) = \sum_{m=1}^{P}\sum_{n=1}^{Q}\Bigg(2\sum_{l_{m,n}=l_{\min}}^{l_{\max}}(l_{m,n}-\mu)^2 \\ -\sum_{l_{m,n}=l_{\min}}^{t-1}(l_{m,n}-\mu_0)^2 - \sum_{l_{m,n}=t}^{l_{\max}}(l_{m,n}-\mu_1)^2\Bigg), \\ \forall t \in [l_{\min}+1 l_{\max}-1], \end{aligned} \tag{29}$$

where μ, μ_0 and μ_1 are the mean intensity values of I, M_0 and M_1. The mean intensity values are calculated as follows:

$$\mu = \frac{\sum_{m=1}^{P}\sum_{n=1}^{Q} l_{m,n}}{N}, \tag{30}$$

$$\mu_0 = \frac{\sum_{m=1}^{P}\sum_{n=1}^{Q}\sum_{l_{m,n}=l_{\min}}^{t_1-1} l_{m,n}}{N_0}, \tag{31}$$

and

$$\mu_1 = \frac{\sum_{m=1}^{P}\sum_{n=1}^{Q}\sum_{l_{m,n}=t_1}^{l_{\max}} l_{m,n}}{N_1}, \tag{32}$$

where N, N_0 and N_1 are the total number of pixels in the image I, class M_0 and class M_1, respectively.

The objective function to obtain the optimal threshold t^* is a maximization problem, which is modeled as follows:

$$\mathrm{TS}_{\mathrm{opt}}(t^*) = \arg \max_{l_{\min} < t < l_{\max}} \mathrm{TS}(t). \tag{33}$$

Let us take the bi-level threshold selection approach and apply it to the multilevel thresholding for K threshold levels. The image I is converted into a partitioned image with $K+1$ classes $(M_0, M_1, ..., M_K)$ using the K threshold levels, which can be expressed as follows:

$$\begin{matrix} M_0 \leftarrow l_{m,n} & \text{if } l_{\min} \le l_{m,n} < t_1 \\ M_1 \leftarrow l_{m,n} & \text{if } t_1 \le l_{m,n} < t_2 \\ \vdots & \vdots \\ M_K \leftarrow l_{m,n} & \text{if } t_K \le l_{m,n} < l_{\max} \end{matrix}, m \in (1,2,...,P) \text{and} n \in (1,2,...,Q), \tag{34}$$

which must satisfy $\cup_{c=0}^{K} M_c = I$.

The TS for the $K+1$ class $(M_0, M_1, ..., M_K)$ partitioned image using the K threshold levels $(t_1, t_2, ..., t_K)$ is defined as follows:

$$\begin{aligned} &\mathrm{TS}(t_1, t_2, ..., t_K) \\ &= \sum_{m=1}^{P}\sum_{n=1}^{Q}\Bigg((K+1)\sum_{l_{m,n}=l_{\min}}^{l_{\max}}(l_{m,n}-\mu)^2 \\ &\quad -\sum_{l_{m,n}=l_{\min}}^{t_1-1}(l_{m,n}-\mu_0)^2 - \sum_{l_{m,n}=t_1}^{t_2-1}(l_{m,n}-\mu_1)^2 \\ &\quad -\cdots - \sum_{l_{m,n}=t_K}^{l_{\max}}(l_{m,n}-\mu_K)^2\Bigg), \end{aligned} \tag{35}$$

where the threshold levels $(t_1, t_2, ..., t_K)$ must satisfy the condition $l_{\min} < t_1 < t_2 < ... < t_K < l_{\max}$, and μ, μ_i are the mean intensity values of I and M_i. The mean intensity value μ_i for class M_i is calculated as follows:

$$\mu_i = \frac{\sum_{m=1}^{P}\sum_{n=1}^{Q}\sum_{l_{x,y}=t_i}^{t_{i+1}-1} l_{m,n}}{N_k}, (\forall i \in [0,K]), \tag{36}$$

where $t_0 = l_{\min}$ and $t_{K+1} = l_{\max}$.

Then the threshold score (TS) based multilevel thresholding objective function to obtain the K number of optimal threshold levels $\left(t_1^*, t_2^*, ..., t_K^*\right)$ is a maximization criterion, which is expressed as follows:

$$\mathrm{TS}_{\mathrm{opt}}\left(t_1^*, t_2^*, ..., t_K^*\right) = \arg \max_{l_{\min} < t_1 < t_2 < \cdots < t_K < l_{\max}} \mathrm{TS}(t_1, t_2, ..., t_K) \tag{37}$$

A graphical picture containing the empirical findings is provided in Figure 1, to ensure the intended research outcomes. In contrast to the previous entropy approaches, the following illustrative notes show how our scheme employs a threshold score to determine the optimal

threshold values. For a greater clarity, theoretical discussions are made explicit in the following paragraph.

It is reiterated that Equations (33) and (37) are the objective functions for the bi-level and the multilevel thresholding. We've picked four standard images from the image processing literature labeled Barbara, Baboon, Columbia, and Plane,[28] all of which are 256×256 pixels in size, and presented in the first column of Figure 1. The plots of TS versus threshold value for bi-level and tri-level thresholding are shown in the second and fourth columns of Figure 1, with the red dot points representing the respective optimal values. The related threshold images are generated and presented in the third and fifth columns of Figure 1 for bi-level and tri-

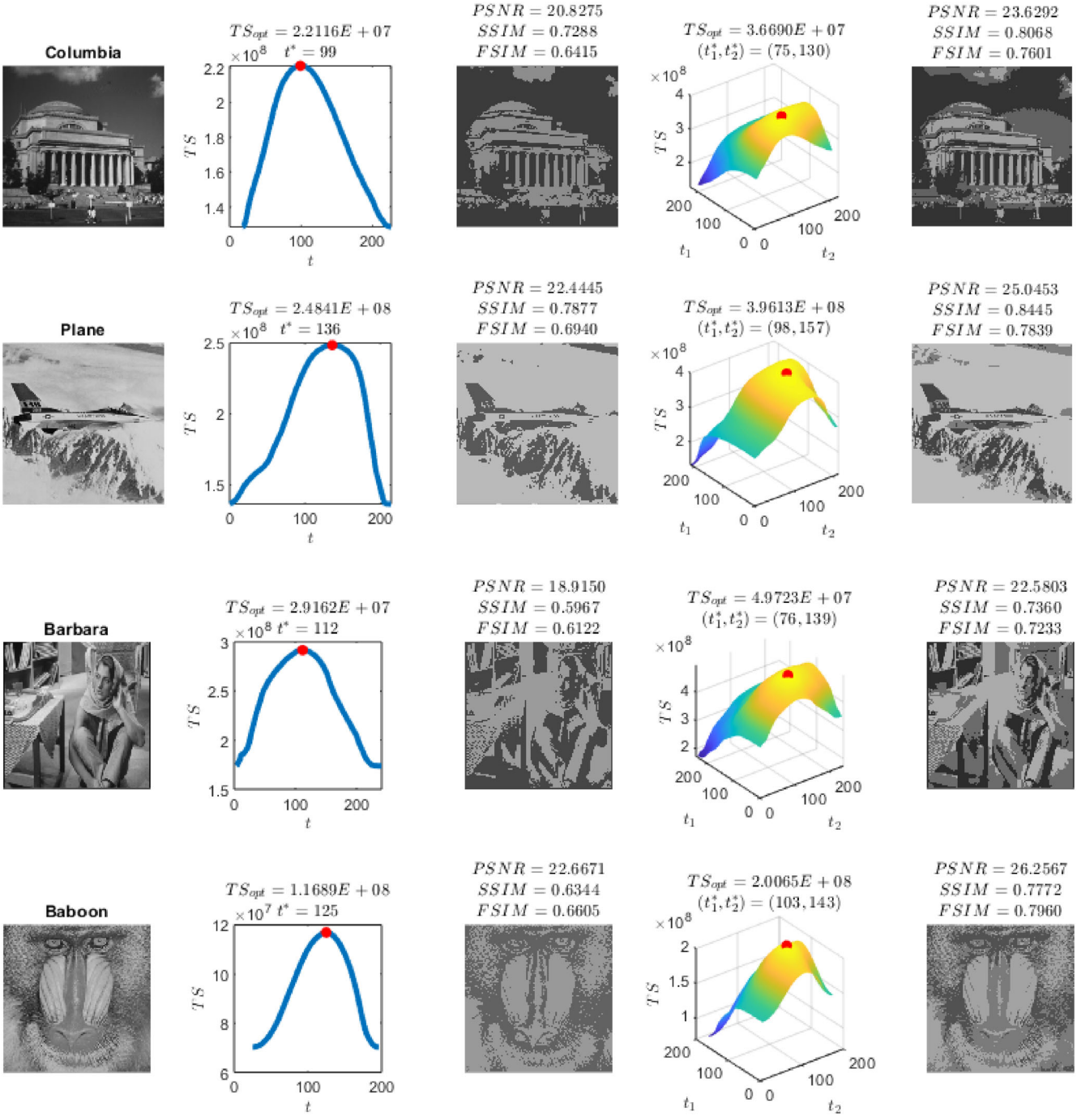

FIGURE 1 Standard images (first column), their threshold scores (second column: bi-level thresholding and fourth column: tri-level thresholding) and the corresponding thresholded images (third column: bi-level thresholded images and fifth column: tri-level thresholded images)

level threshold images, respectively, based on the optimal threshold values. The fifth column tri-level threshold image $(K=2)$ delivers good qualitative and quantitative results than the third column bi-level threshold image $(K=1)$ in Figure 1. The computational complexity to search K optimal threshold values require an exhaustive search of $O\left((l_{\max}-l_{\min}+1)^K\right)$ for a $[l_{\max}-l_{\min}+1]$ distinct gray level within the range $[l_{\min}, l_{\max}]$. The thresholding performance improves as the number of thresholds (K) grows. However, there is a big drawback: the computing time grows exponentially. The most effective way to deal with this is to apply an efficient optimization technique, and hence, the AOSMA is used as an optimizer in these experiments.

4 | A FRAMEWORK OF THE PROPOSED TS-AOSMA METHOD FOR THE OPTIMAL MULTILEVEL THRESHOLDING

In this section, we established the TS-based optimal multilevel thresholding using AOSMA coined as the TS-AOSMA to separate the $K+1$ different class using the K optimal threshold values $\left(t_1^*, t_2^*, \ldots, t_K^*\right)$. The prime objective is to obtain the optimal K threshold values within the range $[l_{\min}+1, l_{\max}-1]$, hence the multilevel thresholding is a K dimensional problem. Considering the TS-based multilevel thresholding is based on the maximizing criterion, AOSMA's purpose is to efficiently

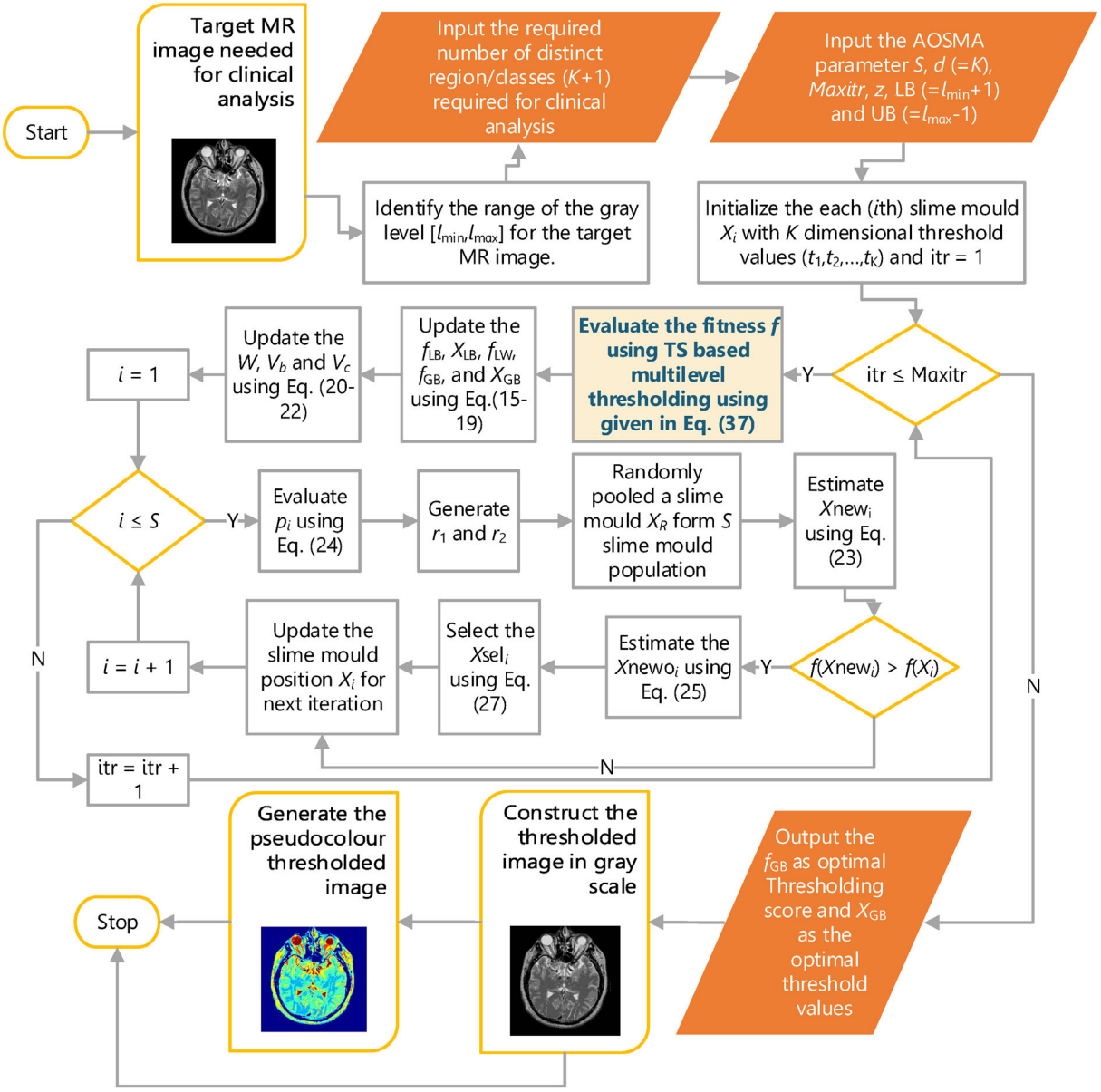

FIGURE 2 Flowchart on the TS-AOSMA method for the optimal multilevel thresholding

maximize it to reduce the computational cost associated with the exhaustive search. The AOSMA began with random initialization of S slime mold positions within the search boundary $[l_{\min}+1, l_{\max}-1]$ for a K-dimensional threshold values $(t_1, t_2, ..., t_K)$. Each slime mold $(X_i, \forall i \in [1, S])$ in the population represents a potential response to a set of threshold values $(t_1, t_2, ..., t_K)$. The slime mold uses the AOSMA described in Section 2.2 to update its population and to reach the global best slime mold X_{GB}. Once the AOSMA reaches the maximum iteration or stopping criteria reached, the X_{GB} represents the K optimal threshold values $\left(t_1^*, t_2^*, ..., t_K^*\right)$. Further, for an interpretation, the optimal threshold values are used to generate the threshold image in pseudo coloring for the clinical analysis and description. A flowchart on the TS-AOSMA method for the optimal multilevel thresholding is presented in Figure 2.

5 | EXPERIMENTAL RESULTS

The main aim is to obtain a suitable MR image with limited, distinct regions of the medical, clinical analysis of the raw MR image with large intensity variations. The limited, distinct region of an image is a threshold image, which is a multilevel thresholding processed image of the original (raw/target) image. In this paper, we propose TS-AOSMA multilevel thresholding to process the target image. We compare the proposed algorithm with other recent works using entropy-based technologies such as Tsallis,[14] Kapur[20] and Masi.[25] This section also provides a discussion on it. Tsallis, Kapur, and Masi multilevel thresholding employing AOSMA are coined as Tsallis-AOSMA, Kapur-AOSMA, and Masi-AOSMA evolutionary approaches of thresholding methods for performance comparison. We used 100 distinct T2-weighted brain MR imaging slices (slice 19 to slice 118) from Harvard Medi-

TABLE 2 Thresholding performance comparison (computed over 100 slices)

K	Metric	TS-AOSMA	Kapur-AOSMA	Tsallis-AOSMA	Masi-AOSMA
2	$\mathrm{PSNR}_{\mathrm{AVE}}$	**24.9624**	17.8858	19.8272	16.9999
	$\mathrm{SSIM}_{\mathrm{AVE}}$	**0.5700**	0.2486	0.2873	0.2241
	$\mathrm{FSIM}_{\mathrm{AVE}}$	**0.7556**	0.6369	0.6517	0.6250
3	$\mathrm{PSNR}_{\mathrm{AVE}}$	**27.4600**	21.7300	24.5056	18.1791
	$\mathrm{SSIM}_{\mathrm{AVE}}$	**0.7285**	0.3813	0.4328	0.2586
	$\mathrm{FSIM}_{\mathrm{AVE}}$	**0.8271**	0.7276	0.7556	0.6606
4	$\mathrm{PSNR}_{\mathrm{AVE}}$	**29.3648**	25.9255	26.7665	20.6007
	$\mathrm{SSIM}_{\mathrm{AVE}}$	**0.8604**	0.5735	0.5384	0.3322
	$\mathrm{FSIM}_{\mathrm{AVE}}$	**0.8763**	0.8106	0.8190	0.7218
5	$\mathrm{PSNR}_{\mathrm{AVE}}$	**31.0505**	28.3442	28.3406	24.7717
	$\mathrm{SSIM}_{\mathrm{AVE}}$	**0.9039**	0.6860	0.6318	0.5245
	$\mathrm{FSIM}_{\mathrm{AVE}}$	**0.9105**	0.8616	0.8556	0.7936

Note: The bold values represent the best results.

Abbreviations: AOSMA, adaptive opposition slime mold algorithm; AVE, average; FSIM, feature similarity index; PSNR, peak signal to noise ratio; SSIM, structure similarity index.

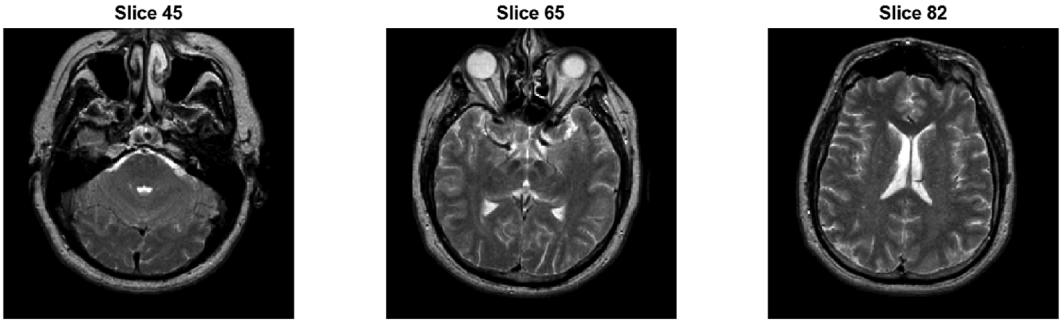

FIGURE 3 Three sample slices 45, 65 and 82 brain magnetic resonance image from AANLIB database

TABLE 3 Optimal threshold value and corresponding performance measure for Slice 45 brain MR image

K	Optimal values	TS-AOSMA	Kapur-AOSMA	Tsallis-AOSMA	Masi-AOSMA
2	TH_{OPT}	44, 121	114, 186	91 175	115, 185
	$PSNR_{OPT}$	**24.1022**	17.0367	19.2679	16.8924
	$SSIM_{OPT}$	**0.5486**	0.2721	0.3200	0.2674
	$FSIM_{OPT}$	**0.7496**	0.5962	0.6232	0.5958
3	TH_{OPT}	30, 81, 133	86, 133, 188	65, 126, 189	103, 148, 189
	$PSNR_{OPT}$	**26.2398**	20.7871	24.0722	18.1414
	$SSIM_{OPT}$	**0.7251**	0.3671	0.4577	0.3036
	$FSIM_{OPT}$	**0.8229**	0.7029	0.7475	0.6558
4	TH_{OPT}	21, 62, 103, 146	28, 72, 124, 185	50, 99, 151, 200	91, 134, 180, 212
	$PSNR_{OPT}$	**28.1674**	27.6836	26.2261	19.8805
	$SSIM_{OPT}$	**0.8558**	0.7360	0.5420	0.3452
	$FSIM_{OPT}$	**0.8755**	0.8424	0.8156	0.6949
5	TH_{OPT}	18, 57, 92, 129, 177	23, 66, 108, 148, 190	42, 84, 126, 168, 211	43, 85, 125, 171, 208
	$PSNR_{OPT}$	**29.8707**	29.4157	27.8213	27.6287
	$SSIM_{OPT}$	**0.8700**	0.8578	0.6014	0.5995
	$FSIM_{OPT}$	**0.8940**	0.8929	0.8514	0.8459

Note: The bold values represent the best results.
Abbreviations: AOSMA, adaptive opposition slime mold algorithm; FSIM, feature similarity index; MR, magnetic resonance; OPT, optimal; PSNR, peak signal to noise ratio; SSIM, structure similarity index; TH, threshold.

TABLE 4 Optimal threshold value and corresponding performance measure for Slice 65 brain MR image

K	Optimal values	TS-AOSMA	Kapur-AOSMA	Tsallis-AOSMA	Masi-AOSMA
2	TH_{OPT}	47, 127	117, 180	90, 173	121, 184
	$PSNR_{OPT}$	**23.4419**	16.2639	18.9880	16.0005
	$SSIM_{OPT}$	**0.5330**	0.3059	0.3419	0.2977
	$FSIM_{OPT}$	**0.6909**	0.5817	0.5973	0.5744
3	TH_{OPT}	40, 100, 152	100, 145, 189	66, 129, 190	102, 145, 191
	$PSNR_{OPT}$	**25.8178**	18.0968	24.1518	17.8708
	$SSIM_{OPT}$	**0.6412**	0.3551	0.4848	0.3506
	$FSIM_{OPT}$	**0.7783**	0.6556	0.7143	0.6515
4	TH_{OPT}	22, 66, 110, 163	95, 138, 180, 222	52, 102, 151, 202	101, 140, 180, 221
	$PSNR_{OPT}$	**27.4668**	18.6620	26.5518	17.9100
	$SSIM_{OPT}$	**0.8363**	0.3684	0.5929	0.3542
	$FSIM_{OPT}$	**0.8263**	0.6766	0.7888	0.6638
5	TH_{OPT}	19, 60, 98, 134, 182	20, 67, 115, 157, 196	42,84, 126, 169, 210	92, 123, 158, 190, 226
	$PSNR_{OPT}$	**29.6209**	28.6048	27.8671	19.3792
	$SSIM_{OPT}$	**0.8666**	0.8428	0.6643	0.3906
	$FSIM_{OPT}$	**0.8727**	0.8557	0.8326	0.7078

Note: The bold values represent the best results.
Abbreviations: AOSMA, adaptive opposition slime mold algorithm; FSIM, feature similarity index; MR, magnetic resonance; OPT, optimal; PSNR, peak signal to noise ratio; SSIM, structure similarity index; TH, threshold.

TABLE 5 Optimal threshold value and corresponding performance measure for Slice 82 brain MR image

K	Optimal values	TS-AOSMA	Kapur-AOSMA	Tsallis-AOSMA	Masi-AOSMA
2	TH_{OPT}	44, 124	111, 169	93, 170	113, 170
	$PSNR_{OPT}$	**23.7733**	16.4348	18.0951	16.3195
	$SSIM_{OPT}$	**0.5701**	0.2787	0.2978	0.2765
	$FSIM_{OPT}$	**0.7157**	0.5872	0.5884	0.5842
3	TH_{OPT}	42, 105, 171	101, 144, 188	68, 128, 189	109, 165, 206
	$PSNR_{OPT}$	**26.2159**	17.3726	24.0319	16.6422
	$SSIM_{OPT}$	**0.6945**	0.3073	0.4317	0.2860
	$FSIM_{OPT}$	**0.7459**	0.6484	0.7015	0.6034
4	TH_{OPT}	34, 83, 119, 180	95, 132, 168, 208	56, 105, 155, 204	101, 144, 178, 212
	$PSNR_{OPT}$	**28.1922**	18.1426	26.7104	17.3972
	$SSIM_{OPT}$	**0.7373**	0.3250	0.5590	0.3093
	$FSIM_{OPT}$	**0.8325**	0.6778	0.7692	0.6545
5	TH_{OPT}	19, 58, 92, 127, 187	10, 62, 115, 167, 207	44, 86, 128, 171, 213	93, 123, 157, 188, 219
	$PSNR_{OPT}$	**29.9791**	28.2101	28.4173	18.4681
	$SSIM_{OPT}$	**0.8637**	0.8753	0.6492	0.3327
	$FSIM_{OPT}$	**0.8721**	0.8084	0.8335	0.6923

Note: The bold values represent the best results.

Abbreviations: AOSMA, adaptive opposition slime mold algorithm; FSIM, feature similarity index; MR, magnetic resonance; OPT, optimal; PSNR, peak signal to noise ratio; SSIM, structure similarity index; TH, threshold.

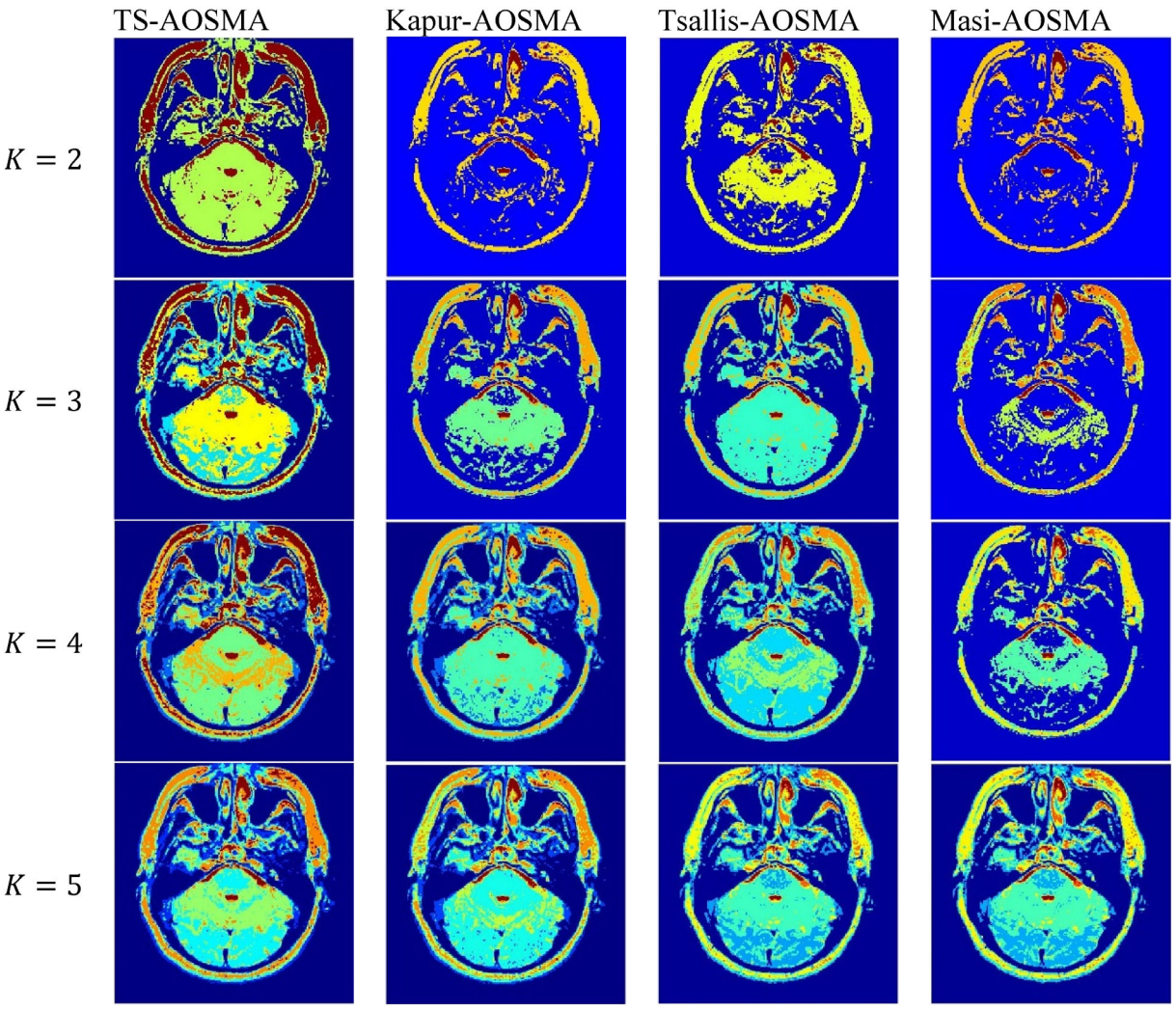

FIGURE 4 Threshold images for Slice 45 brain magnetic resonance image

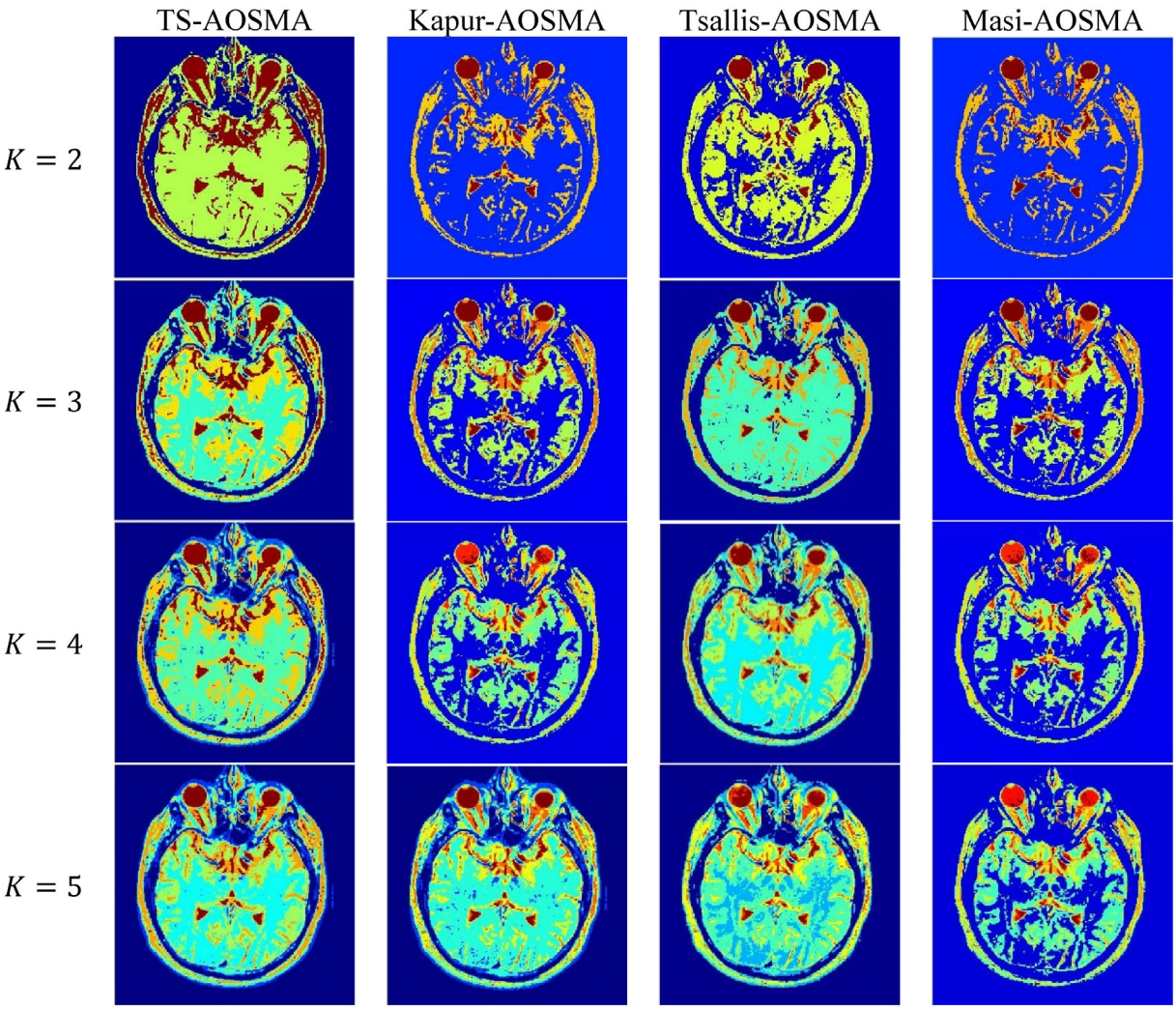

FIGURE 5 Threshold images for Slice 65 brain magnetic resonance image

cal School's whole brain atlas dataset[22] for the experimental purposes in this paper. Gray scale images are considered for the experiment.

In our experiments, the first simple and effective performance metric uses as Peak Signal to Noise Ratio (PSNR),[25] which is evaluated as follows:

$$\mathrm{PSNR(db)} = 10\log 10\left(\frac{255^2}{\mathrm{MSE}\left(I,\hat{I}\right)}\right), \tag{38}$$

where MSE (mean square error) between $P \times Q$ dimensional target image I intensity value $l_{m,n}$ and thresholded image $\hat{I}$ intensity value $\hat{l}_{m,n}$ is

$$\mathrm{MSE} = \frac{1}{P \times Q}\sum_{m=1}^{P}\sum_{n=1}^{Q}\left(l_{m,n} - \hat{l}_{m,n}\right)^2. \tag{39}$$

As PSNR is a signal-to-noise ratio, a higher value PSNR suggests that the thresholded image has more information and less noise. The second performance metric based on structure, contrast and brightness is Structure Similarity Index Measure (SSIM)[29] with a larger SSIM value indicating a better-thresholded image. The third performance metric based on the gradient magnitude map and the phase congruency map is Feature Similarity Measure (FSIM)[30] an image quality assessment index. For a better-threshold image, a high FSIM value is preferred.

To make consistency among the experiments on evolutionary multilevel thresholding TS-AOSMA, Tsallis-AOSMA, Kapur-AOSMA and Masi-AOSMA methods run for 200 maximum iterations with 30 slime mold as a population count. The Tsallis parameter q is chosen as 0.1 and the Masi parameter r is chosen as 0.5 for the evolutionary multilevel thresholding method Tsallis-AOSMA and Masi-AOSMA, respectively. Each target MR image from 100 slices is subjected to 11 independent runs of the evolutionary multilevel thresholding technique for the threshold levels $K = 2, 3, 4, 5$. To show the effectiveness of

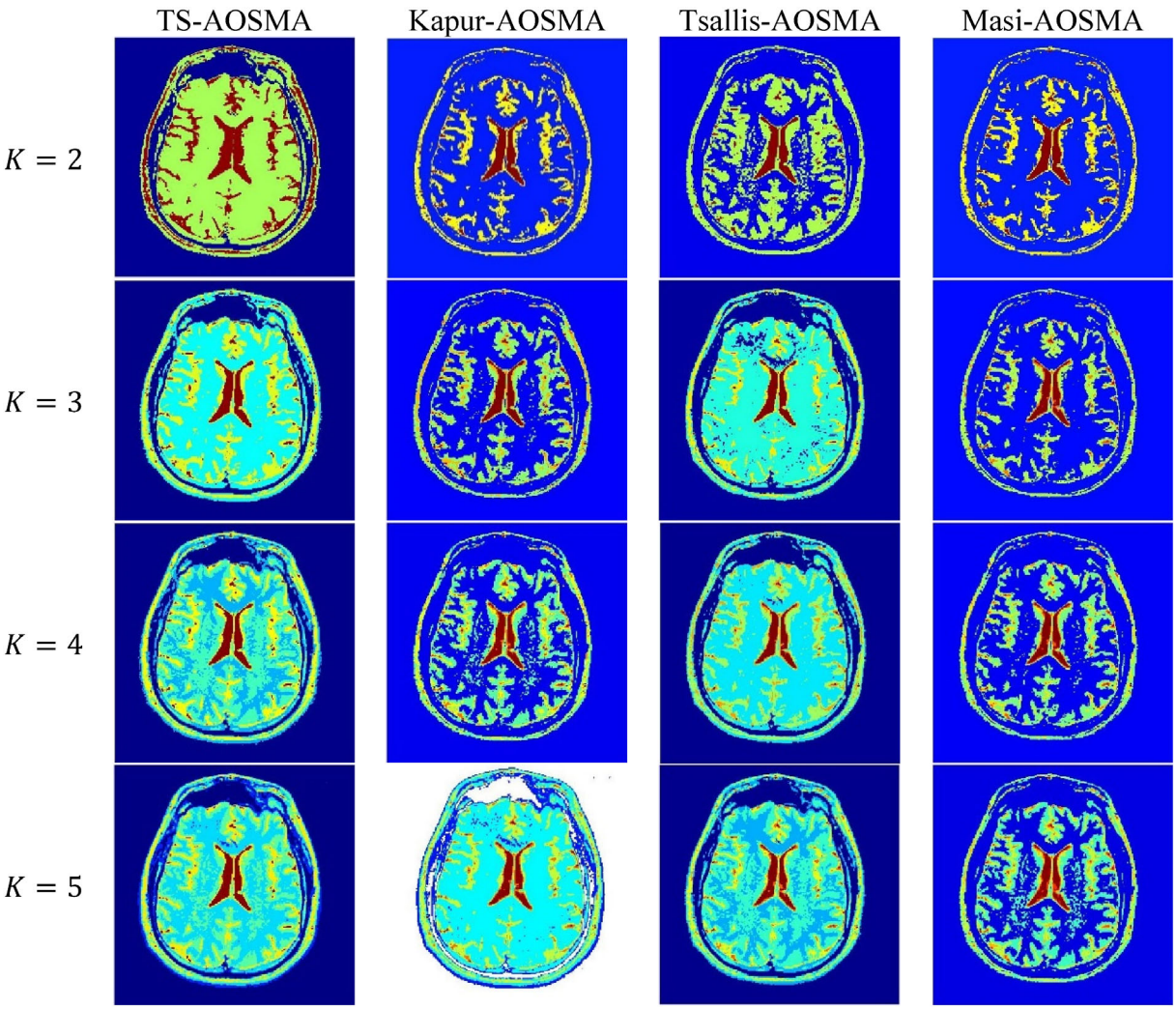

FIGURE 6 Threshold images for Slice 82 brain magnetic resonance image

the proposed methods over 100 slice brain MR images, a thresholding performance comparison using average PSNR ($PSNR_{AVE}$), average SSIM ($SSIM_{AVE}$) and average FSIM($FSIM_{AVE}$) is presented in Table 2. From Table 2, the average performance of the TS-based approach outperforms Kapur, Tsallis and Masi-based techniques. It should also be noted from Table 2 that as threshold values are elevated, PSNR, SSIM, and FSIM performance improves.

To provide depth analysis on the performance of proposed TS-AOSMA methods to others Slice 45, 65 and 82 brain MR images are considered for experiments. These sample gray scale brain MR images are presented in Figure 3. The performance comparisons are done with the optimal PSNR ($PSNR_{OPT}$), optimal SSIM ($SSIM_{OPT}$) and optimal FSIM ($FSIM_{OPT}$) obtained using the threshold image generated with an optimal threshold value (TH_{OPT}). The improved results depend primarily on the appropriate value of the threshold. The optimizer AOSMA is employed to lower computing costs in this case, but the role of the multilevel thresholding fitness function is crucial. The inherent characteristics of the images and parameters connected with the multilevel thresholding fitness function may also have an impact on the findings. Some results are offered here for justification in this context.

The optimal threshold value and corresponding performance measures of brain MR images are presented in Table 3 for slice 45, Table 4 for slice 65 and Table 5 for slice 82. The evolutionary TS-AOSMA outperforms other methods in all experimented threshold levels $K = 2, 3, 4, 5$. Outputs (segmented MRI) are shown (Figures 4-6) using pseudo coloring, for a better visual representation. For instance, when $K = 5$, we see $K + 1$, i. e 6 segments (six different colors). The respective threshold image from Table 3 is exhibited in Figure 4, Table 4 is shown in Figure 5 and Table 5 is shown in Figure 6. In all the experimented threshold levels $K = 2, 3, 4, 5$, it can

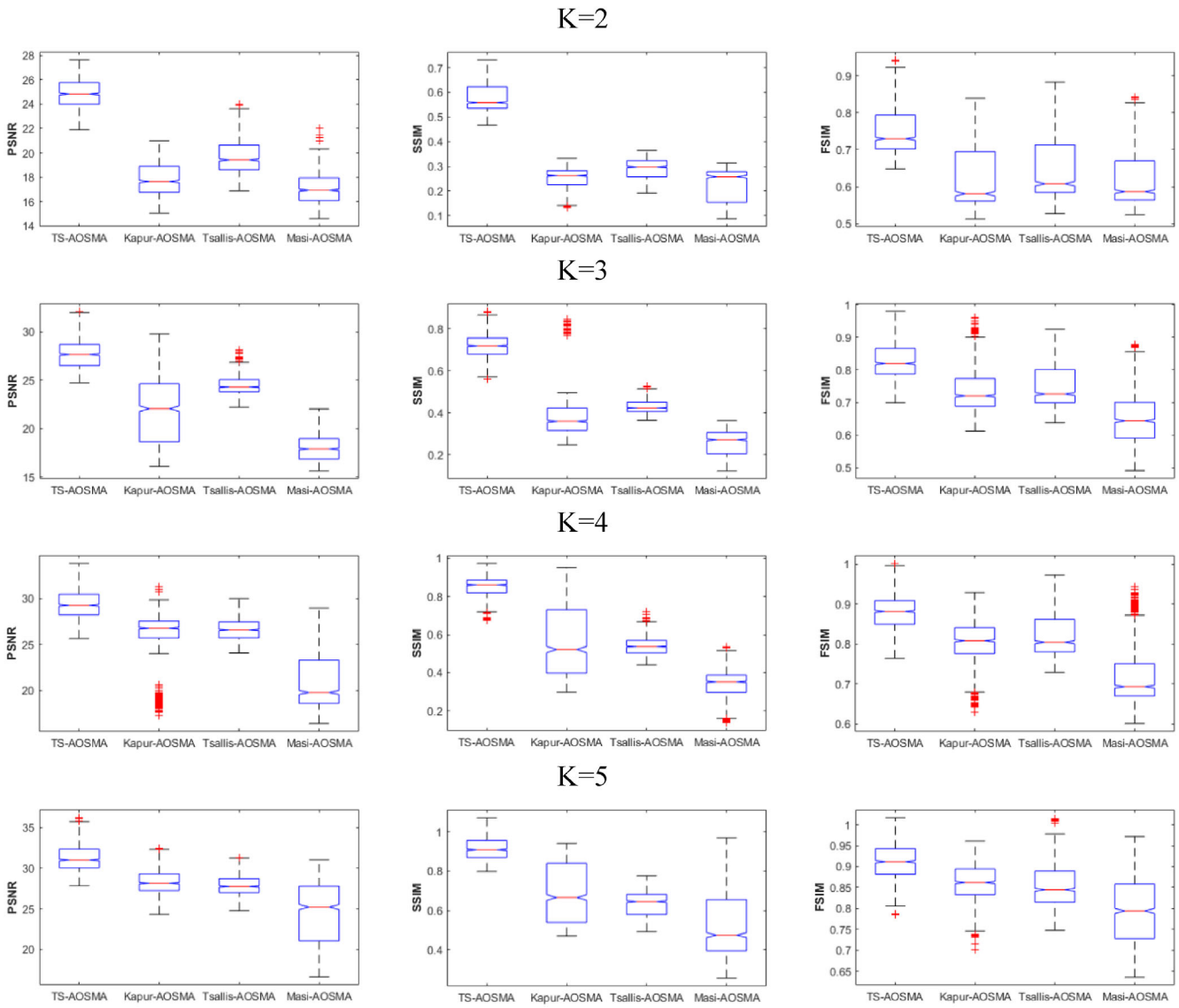

FIGURE 7 ANOVA test result of each method computed over 100 slices

be observed that the TS-AOSMA produces superior results than the other methods Kapur-AOSMA, Tsallis-AOSMA, and Masi-AOSMA. The performance of TS-AOSMA is consistent for low $(K=2)$ and progressive $(K=3,4,5)$ threshold levels based on the performance measure and thresholded image. This investigation shows that TS-based multilevel thresholding has some promising possibilities in the field of image processing segmentation.

The ANOVA statistical test (as boxplots) is used to measure the multilevel thresholding methods. These methods are implemented to further study the TS-AOSMA based approach. To perform the ANOVA statistical test, here 1100 data samples are used. These are the outcomes of 11 independent runs of each 100 slices (slice 19 to slice 118) used for the experiments. The ANOVA test results are shown in Figure 7. Separate boxplots are drawn for each performance metric such as PSNR, SSIM and FSIM, to the threshold level $K = 2, 3, 4$ and 5. The height of the boxplot exhibits the consistency of the method. Less height means low noise (low standard deviation). From Figure 7, it is observed that the TS-AOSMA has shown more consistency in terms of the height of the boxplot, when compared with the other methods. As we know, the higher the value of the performance metric, the method shows more prominent result, in multilevel thresholding. From Figure 7, it is revealed that the TS-AOSMA has shown promising results as opposed to other methods—Kapur-AOSMA, Tsallis-AOSMA and Masi-AOSMA. The proposal may be useful for classification.[31]

6 | CONCLUSIONS

This paper proposed a new non-entropy-based multilevel thresholding method. The critical facts are highlighted in this section. The proposal is histogram independent, as opposed to the existing technologies that depend on the histogram distribution while computing the entropy values. The proposed technology is a maximization problem. The TS-based procedure uses pixels' intensity values and an average intensity value in a class that is not based on the pixel distribution in an image. It is our method's intrinsic property. This non-entropic TS method more effectively senses the intensity variation in an image. This paper, therefore, presents evolutionary multilevel thresholding for the brain MR images using the AOSMA. The TS-based objective function is used to compute the optimal thresholds. The findings are evaluated using the performance measures of the proposed evolutionary TS-AOSMA. Nonetheless, it suggests its effectiveness in the brain MR image thresholding. The quantitative and qualitative findings demonstrate that the proposed TS-AOSMA method outperforms the Tsallis-AOSMA, Kapur-AOSMA and Masi-AOSMA. From Table 2, the claims of the proposal are implicit. To figure out—(i) The PSNR values achieved are higher by 20.19%, 13.47%, and 40.08% with respect to Tsallis, Kapur and Masi techniques, respectively; (ii) The SSIM values yielded are higher by 62.10%, 62.03%, and 128.67% as compared to Tsallis, Kapur and Masi methods, respectively; (iii) The FSIM values obtained are higher by 20.70%, 14.23%, and 40.83% compared to Tsallis, Kapur and Masi techniques, respectively. Similarly, significant improvements are achieved for three different slices, results are shown in Tables 2–4. Exemplary results achieved reveal the fact that our technology is efficient for brain MR image segmentation. The limitation of our study may be the problem of over-segmentation, when the number of threshold levels is very high, say $K = 10$ or higher. This may be explored in the future. This limitation may be due to the inherent characteristics of the brain MR images or may be due to the limitation of our technology.

Multilevel thresholded MRI is commonly in use for measuring and visualizing dissimilar brain assemblies, for outlining lesions, for extracting brain features, for image-guided instructions and surgical planning. Nevertheless, it is unquestionable that computerized multiclass segmentation technologies have shown their potential for use in computer-aided diagnosis/therapy planning. The suggested work would give the multilevel medical image thresholding field a new direction. The proposed methodology may also be used to evaluate other imaging modalities like CT, PET, X-Ray etc., where we find the intensity variations. The future scope of this work is to extend the idea for color segmentation, satellite image denoising, breast thermogram thresholding and image classification with many more computer vision applications.

ACKNOWLEDGMENT

This research has been financially supported by The Analytical Center for the Government of the Russian Federation (Agreement No. 70-2021-00143 dd. 01.11.2021, IGK000000D730321P5Q0002).

CONFLICT OF INTEREST

The authors declare no conflict of interest.

DATA AVAILABILITY STATEMENT

The standard images are taken from http://www.dip.ee.uct.ac.za/imageproc/stdimages/greyscale/ [28] and MR images are taken from the whole barin atlas dataset of Harvard medical school and found in: https://www.med.harvard.edu/aanlib/home.html [22].

ORCID

Rutuparna Panda https://orcid.org/0000-0002-8676-0144

REFERENCES

1. Maitra M, Chatterjee A. A novel technique for multilevel optimal magnetic resonance brain image thresholding using bacterial foraging. *Measurement*. 2008;41(10):1124-1134. doi:10.1016/j.measurement.2008.03.002
2. Xue G, Chen C, Lu Z-L, Dong Q. Brain imaging techniques and their applications in decision-making research. *Xin Li Xue Bao*. 2010;42(1):120-137. doi:10.3724/SP.J.1041.2010.00120
3. Saritha S, Amutha Prabha N. A comprehensive review: segmentation of MRI images—brain tumor. *Int J Imaging Syst Technol*. 2016;26(4):295-304. doi:10.1002/ima.22201
4. Sezgin M, Sankur B. Survey over image thresholding techniques and quantitative performance evaluation. *J Electron Imaging*. 2004;13(1):146-168. doi:10.1117/1.1631315
5. Sankur B, Sezgin M. Image thresholding techniques: a survey over categories. *Pattern Recognit*. 2001;34:1573-1583.
6. Zaitoun NM, Aqel MJ. Survey on image segmentation techniques. *Procedia Comput Sci*. 2015;65:797-806. doi:10.1016/j.procs.2015.09.027
7. Otsu N. A threshold selection method from gray level histograms. *IEEE Trans Syst Man Cybern*. 1979;9:62-66. doi:10.1109/TSMC.1979.4310076
8. Kannappan P. On Shannon's entropy, directed divergence and inaccuracy. *Zeitschrift für Wahrscheinlichkeitstheorie Und Verwandte Gebiete*. 1972;22(2):95-100. doi:10.1007/BF00532728
9. Portes de Albuquerque M, Esquef IA, Gesualdi Mello AR, Portes de Albuquerque M. Image thresholding using Tsallis entropy. *Pattern Recognit Lett*. 2004;25(9):1059-1065. doi:10.1016/j.patrec.2004.03.003
10. Kapur JNN, Sahoo PKK, Wong AKCKC. A new method for gray-level picture thresholding using the entropy of the

histogram. *Comput Vision Graph Image Process*. 1985;29(3):273-285. doi:10.1016/0734-189X(85)90125-2
11. Li CH, Lee CK. Minimum cross entropy thresholding. *Pattern Recognit*. 1993;26(4):617-625. doi:10.1016/0031-3203(93)90115-D
12. Masi M. A step beyond Tsallis and Rényi entropies. *Phys Lett Sect A Gen Solid State Phys*. 2005;338(3–5):217-224. doi:10.1016/j.physleta.2005.01.094
13. Yin P-Y. A fast scheme for optimal thresholding using genetic algorithms. *Signal Processing*. 1999;72(2):85-95. doi:10.1016/S0165-1684(98)00167-4
14. Rajinikanth V, Satapathy SC, Fernandes SL, Nachiappan S. Entropy based segmentation of tumor from brain MR images – a study with teaching learning based optimization. *Pattern Recognit. Lett.* 2017;94:87-95. doi:10.1016/j.patrec.2017.05.028
15. Oliva D, Hinojosa S, Cuevas E, Pajares G, Avalos O, Gálvez J. Cross entropy based thresholding for magnetic resonance brain images using crow search algorithm. *Expert Syst Appl*. 2017;79:164-180. doi:10.1016/j.eswa.2017.02.042
16. Sathya PD, Kayalvizhi R. Optimal segmentation of brain MRI based on adaptive bacterial foraging algorithm. *Neurocomputing*. 2011;74(14):2299-2313. doi:10.1016/j.neucom.2011.03.010
17. Manikandan S, Ramar K, Willjuice Iruthayarajan M, Srinivasagan KG. Multilevel thresholding for segmentation of medical brain images using real coded genetic algorithm. *Measurement*. 2014;47:558-568. doi:10.1016/j.measurement.2013.09.031
18. Kaur T, Saini BS, Gupta S. A joint intensity and edge magnitude-based multilevel thresholding algorithm for the automatic segmentation of pathological MR brain images. *Neural Comput Appl*. 2018;30(4):1317-1340. doi:10.1007/s00521-016-2751-4
19. Gtifa W, Hamdaoui F, Sakly A. 3D brain tumor segmentation in MRI images based on a modified PSO technique. *Int J Imaging Syst Technol*. 2019;29(4):501-509. doi:10.1002/ima.22328
20. Kotte S, Pullakura RK, Injeti SK. Optimal multilevel thresholding selection for brain MRI image segmentation based on adaptive wind driven optimization. *Measurement*. 2018;130:340-361. doi:10.1016/j.measurement.2018.08.007
21. Naik MK, Panda R, Abraham A. Adaptive opposition slime mould algorithm. *Soft Comput*. 2021;25:14297-14313. doi:10.1007/s00500-021-06140-2
22. The Whole Brain Atlas. Accessed August 15, 2021. https://www.med.harvard.edu/aanlib/home.html.
23. Lim KO, Pfefferbaum A. Segmentation of MR brain images into cerebrospinal fluid spaces, white and gray matter. *J Comput Assist Tomogr*. 1989;13(4):588-593. doi:10.1097/00004728-198907000-00006
24. Agrawal S, Panda R, Bhuyan S, Panigrahi BK. Tsallis entropy based optimal multilevel thresholding using cuckoo search algorithm. *Swarm Evol Comput*. 2013;11:16-30. doi:10.1016/j.swevo.2013.02.001
25. Khairuzzaman AK, Chaudhury S. Masi entropy based multilevel thresholding for image segmentation. *Multimed Tools Appl*. 2019;78:33573-33591. doi:10.1007/s11042-019-08117-8
26. Li S, Chen H, Wang M, Heidari AA, Mirjalili S. Slime mould algorithm: a new method for stochastic optimization. *Futur Gener Comput Syst*. 2020;111:300-323. doi:10.1016/j.future.2020.03.055
27. Tizhoosh H. R.. Opposition-based learning: A new scheme for machine intelligence. Paper presented at International Conference on Computational Intelligence for Modelling, Control and Automation and International Conference on Intelligent Agents, Web Technologies and Internet Commerce (CIMCA-IAWTIC'06), 2005, 1, pp. 695–701, doi: 10.1109/CIMCA.2005.1631345
28. "Greyscale Standard Images." Accessed August 26, 2021. http://www.dip.ee.uct.ac.za/imageproc/stdimages/greyscale/.
29. Zhou W, Bovik AC, Sheikh HR, Simoncelli EP. Image quality assessment: from error visibility to structural similarity. *IEEE Trans Image Process*. 2004;13(4):600-612. doi:10.1109/TIP.2003.819861
30. Lin Zhang LZ, Zhang L, Zhang L, Mou X, Zhang D, Lin Zhang LZ. FSIM: a feature similarity index for image quality assessment. *IEEE Trans Image Process*. 2011;20(8):2378-2386. doi:10.1109/TIP.2011.2109730
31. Protasov S, Khan AM. Using proximity graph cut for fast and robust instance-based classification in large datasets. *Complexity*. 2021;2011738. doi:10.1155/2021/2011738

How to cite this article: Naik MK, Panda R, Samantaray L, Abraham A. A novel threshold score based multiclass segmentation technique for brain magnetic resonance images using adaptive opposition slime mold algorithm. *Int J Imaging Syst Technol*. 2022;1-17. doi:10.1002/ima.22713